JCEC
THE JOURNAL OF ENGINEERING AND EXACT SCIENCES

OPEN ACCESS

The Journal of Engineering and Exact Sciences – jCEC, Vol. 07 N. 04 (2021)
journal homepage: https://periodicos.ufv.br/ojs/jcec
ISSN: 2527-1075

Multi-response optimization of EDM drilling parameters of the Nitinol SMA

Otimização de múltiplas respostas de parâmetros de perfuração EDM do Nitinol SMA

Article Info:
Article history: Received 2021-07-20 / Accepted 2021-08-16/ Available online 2021-08-16
doi: 10.18540/jcecvl7iss4pp13007-01-17e

Amiya Kumar Sahoo
ORCID: https://orcid.org/0000-0001-6572-4438
Jaypee University of Engineering and Technology, India
E-mail: amiya.badani@gmail.com
Praneet Pandey
ORCID: https://orcid.org/0000-0003-1070-1727
Jaypee University of Engineering and Technology, India
E-mail: pandeypraneet@gmail.com
Dhananjay R Mishra
ORCID: https://orcid.org/0000-0002-5107-0012
Jaypee University of Engineering and Technology, India
E-mail: dm30680@gmail.com

Resumo
A demanda por Nitinol (SMA) está aumentando rapidamente para várias aplicações. Com o objetivo de otimizar os parâmetros de controle de EDM, 46 experimentos foram concluídos em seis corpos de prova de 6,156 mm de espessura usando a máquina de perfuração EDM Sparkonix. Corrente (I), tensão (V), tempo de carga (T_{ON}), tempo de descarga (T_{OFF}) e pressão dielétrica (DP) foram tomados como parâmetros de controle de entrada. A otimização de índice único da taxa de remoção de material (MRR), taxa de desgaste da ferramenta (TWR) e grau de rosqueamento (DoT) são avaliados usando o grau relacional cinza (GRG). Contribuições de parâmetros de controle individuais são avaliadas usando Taguchi e ANOVA. Os parâmetros de controle de entrada ótimos obtidos foram usados para o experimento de confirmação, e o resultado obtido dá uma boa concordância com ele. V e T_{ON} são encontrados como os parâmetros mais significativos. Os valores máximo e mínimo de MRR, TWR e DoT foram registrados como 0,0277 e 0,0074 g / min, 0,0177 e 0,0033 g / min e 0,032 e 0,01 radianos, respectivamente. MRR, TWR e DoT melhoraram em 49,1, 4,5 e 43,3%, respectivamente.
Palavras-chave: EDM. Nitinol. Eletrodo tubular rotativo de cobre. GRA. Taguchi.

Abstract
The demand for Nitinol (SMA) is increasing rapidly for various applications. With the aim of optimum control parameters of EDM, 46 experiments completed on six specimens of 6.156 mm thickness using Sparkonix EDM drill machine. Current (I), voltage (V), charging-time (T_{ON}), discharging-time (T_{OFF}), and dielectric pressure (DP) were taken as input control parameters. Single-indexed optimization of material removal rate (MRR), tool-wear rate (TWR), and degree of tapperness (DoT) are evaluated using gray relational grade (GRG). Individual control-parameter contributions are evaluated using Taguchi and ANOVA. The obtained optimal input control parameters were used for the confirmation experiment, and the obtained result gives good agreement to it. V and T_{ON} are found as the most significant parameters. Maximum and minimum values of MRR, TWR, and DoT have been recorded as 0.0277 & 0.0074 g/min, 0.0177 & 0.0033 g/min, and 0.032 & 0.01 radians respectively. MRR, TWR, and DoT improved by 49.1, 4.5, and 43.3 %, respectively.
Keywords: EDM. Nitinol. Copper rotary tubular electrode. GRA. Taguchi.

Nomenclature

DP	dielectric pressure (kg/cm^2)
I	discharge current (A)
T_{ON}	pulse on time (μs)
T_{OFF}	pulse off time (μs)
V	gap voltage (V)
ANOVA	analysis of variance
DoT	degree of tapperness (rad)
EDM	electric discharge machining
GRA	gray relational analysis
GRG	gray relational grade
MRR	material removal rate (g/min)
SNR	signal to noise ratio (db)
TWR	tool wear rate (g/min)

1. Introduction

The EDM machining process has become famous and vital due to its numerous applications in different industries (viz. aerospace, automotive, power plant) and its ability to produce precise, axisymmetry and arbitrary shapes electrically conductive materials. As EDM has high initial and operating costs, it needs to be operated on the parameters that give the desired unique quality at minimum manufacturing time and cost for shortening payback.

Productivity and quality will get affected due to the selection of inappropriate control parameters; hence, the choice of optimal control parameters is one of the significant concerns for the manufacturing industry. The selection of optimum control parameters depends on the machine and material. The most crucial process control parameters that affect the EDM drilling process largely are dielectric pressure, gap voltage, discharge current, and type of electrode. Many researchers have reported optimising electrode wear rate, material removal rate, hole circularity, and taper angle for different materials on EDM (P. Sharma et al., 2014; Shin et al., 2019). Process selection and evaluation of non-traditional machining using the generation of the standard through-hole in glass and deep through cavities in titanium with the integration of roughness number by using multi-attribute border approximation area comparison method for seventeen different machines has been reported by Chakraborty et al. (2019).

Effect on mechanical properties of Nitinol (medical grade) and characterization (arcing phenomena) in micro-EDM has been reported by Mwangi et al. (2020). They have reported that the three peak-transformation behaviour arcing phenomena will play a vital role, and thermal damage caused by arcing enhances residual strain, minimizes elongation to failure, machining accuracy, and lower and upper plateau stresses. Liu et al. (2018) conducted wire-EDM on Nitinol SMA and found that a thin white layer with less residual tensile stress slows down the crack formation and propagation, enhancing fatigue life. K. E. Ch. Vidyasagar et al. (2020) reported improvement of corrosion resistance of Nitinol in the presence of simulated body fluid by depositing titanium oxides on its surface. Nguyen HuuPhan et al. (2020) reported an evenly distributed white layer using titanium power with the dielectric fluid and copper electrode as the electrode's electrical and thermal conductivity, and the powder affects the surface quality.

Himadri Majumder and Kalipada Maity (2018) optimized process parameters of WEDM of Nitinol for surface roughness and micro-hardness by using general regression neural network and fuzzy logic. Shape memory behaviour of Nitinol is a thermo-mechanical phase transformation between the martensitic and austenitic phases. In micro-EDM, the high energy dissipated for material removal can significantly change the SMA phase transformation behaviour to reduce thermal hysteresis (Mwangi et al., 2018). Kannan et al. (2018) compared different post-heat

treatment processes on the laser-welded Nitinol sheet and found that laser processing has a lower difference in phase transformation temperature due to self-quenching and controlled heat input. Major input variable factors influencing the performance characteristics of WEDM for Nimonic-75 alloy based on principal component evaluation and Taguchi and ANOVA analysis have been reported by Sonawane and Kulkarni (2018). They reported improvement in the composite primary component from 1.2013 to 1.2443 in multiple-response at optimal machining process parameters. Optimization of process parameters for powder mixed electro-discharge machining using the technique for order of preference by similarity to ideal solution (TOPSIS) and GRA has been reported by Tripathy and Tripathy (2016).

Md Al-Amin et al. (2020) reviewed power mixed EDM for biomedical applications to improve surface quality by depositing some superior metal to enhance the material's micro-hardness and corrosion resistance property. Singh et al. (P. N. Singh et al., 2004) have reported optimization of EDM parameter by using GRA for machining of Al - 10% SiCp composite. Lin and Lin (2002) have utilized GRA to optimise EDM process parameters using the orthogonal array considering gray relational grade as a performance index. Sudhir Kumar et al. (S. Kumar et al., 2020) reported multi-performance characteristics of die-sinking EDM improved using Taguchi-GRA technique and growth of 0.0860 in GRG on AISI420 stainless steel.

Ramver Singh et al. (2020) investigated EDMed deep micro-holes on Ti-6Al-4V alloy and reported the size of debris reduced and the increase in the size of gas bubbles along with the depth of the hole. Ahmed et al. (2019) have reported the deep-hole drilling method of Inconel 718 material to analyze the effectiveness of coolant pressure and rotational speed on the hole's straightness during the process using Euler-Bernoulli beam theory.

Ankit Sharma et al. (2020) reported deposition of Inconel 718 on the surface of aluminium alloy 7075 using the EDM process, which enhanced the micro-hardness to 1.5 to 2.5 times. A detailed review of the micro and conventional EDM machining process for tungsten carbide and its composite material has been reported by Jahan et al. (2011). Kumar et al. (2020) extensively reviewed the micro-EDM process concerning discharge power and dielectric circulation and its sustainability system for green manufacturing. The machinability of Nitinol shape memory alloy (SMA) is inadequate for its lower thermal conductivity and work hardening effect leading to higher cutting zone temperature in conventional machining conditions (A. Sharma & Yadava, 2018).

Therefore, unconventional methods of material removal supersede traditional methods. EDM drilling method can produce micro-holes on hard to cut materials such as Nitinol SMA. In this paper, multi-response optimization of variable control parameters for EDM drilling operation using GRA assisted Taguchi on Nitinol is reported.

2. Material and methods

The two-phased methodology selected to carry out the optimization of variable control parameters of the machining operation of Nitinol SMA is shown in Figure 1. In the first phase, the selection of machining parameters, pilot experiments, and design of experiments using Box-Behnken design (BBD) was carried out. Whereas in the second phase, mathematical modelling, validation of the developed model, ANOVA analysis, confirmation experiments based on optimal results, and percentage contribution of control parameters has been carried out with the help of Taguchi assisted gray relation analysis.

Nitinol is a well-recognized material for its superelasticity and biocompatibility as it has numerous applications in different industries. The material Nitinol used for the experimentation chemically consists of 49.1 % Ni and 50.9 % Ti. The physical and mechanical properties of Nitinol SMA are tabulated in Table 1, respectively.

Table 1 - Physical and mechanical Properties of Nitinol.

Melting Temperature	1240 – 1310 °C
Resistivity (high temperature state)	82 μΩ-cm
Resistivity (low temperature state)	76 μΩ-cm
Thermal Conductivity	0.1 W/cm/°C
Heat Capacity	0.077 cal/gm/°C
Latent Heat	5.78 cal/gm
Magnetic Susceptibility (high temperature)	3.8 μemu/gm
Magnetic Susceptibility (low temperature)	2.5 μemu/gm
Tensile Strength	Austenite: 195 – 690 MPa Martensite: 70 – 140 MPa
Young's Modulus	Austenite: 83 GPa Martensite: 28 – 41 GPa
Density	6.45 g/cm^3

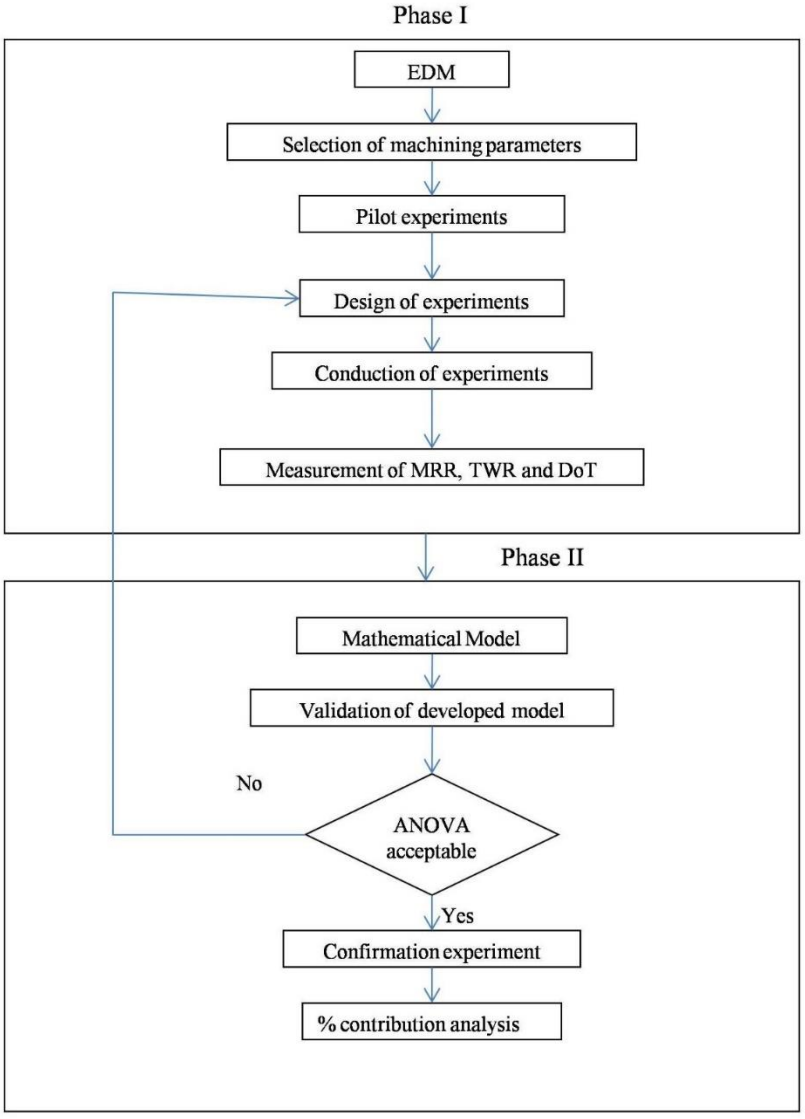

Figure 1 - Phase diagram of the methodology.

The machinability of Nitinol is low due to its mechanical and physical properties. Hence nonconventional machining processes have mostly been taken into account for different material removal operations. All designed experiments were carried out of this study using Sparkonix EDM Drill Speed I machine. Its actual photograph is shown in Figure 2. Technical specifications and details of the EDM machine are tabulated in Table 2. The machine's process parameters have ten steps to control gap voltage, pulse-on time, and pulse-off time, whereas the discharge current has 25-steps of one ampere each.

Figure 2 - Actual photograph of Sparkonix EDM Drill Speed I.

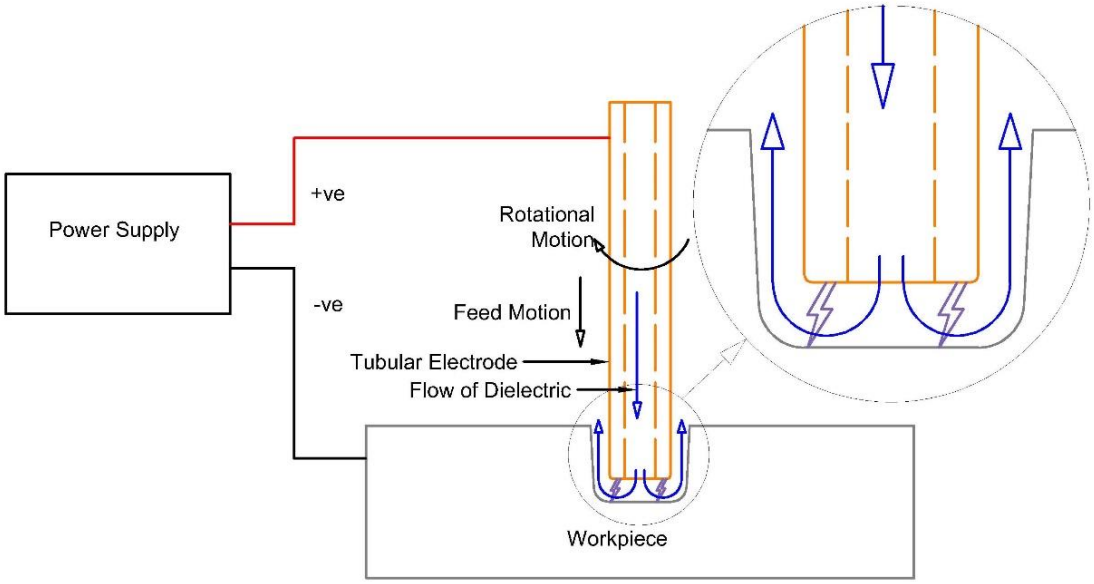

Figure 3 - Schematic of EDM drilling process.

Table 2 - Technical specifications of Sparkonix EDM Drill Speed I.

Sl. No.	Parameter	Range
1	Gap Voltage	10 – 100 V
2	Discharge Current	1 – 25 A
3	Pulse-on Time	1 – 10 μs
4	Pulse-off Time	1 – 10 μs
5	Flushing Pressure	Up to 100 kg/cm^2

The EDM drilling operation would be well understood in Figure 3. The machine has a servo feeding mechanism for the electrode, controlled by the servo reference voltage to maintain the inter-electrode gap. Pilot experiments have been carried out for deciding the different levels of variable control parameters of EDM. Three different current, gap voltage, pulse-on & -off times, and dielectric pressure, are selected and tabulated in Table 3 based on pilot experiments results. Design of experiments reduces the cost and time of experimentation by reducing the redundant combinations of experiments of the full-factorial design and does not compromise the response's quality. BBD is suitable for the nonlinear behaviour of the response, which reduces the number of experiments compared to the full-factorial design and makes the experimentation economical. In the BBD design, a total of forty-six experiments with six replications of the centre point for five input parameters (viz. discharge current, gap voltage, pulse-on & -off times, and dielectric pressure) was carried out using Minitab 17 software.

Table 3 - EDM drilling process parameters with their levels.

Control Factors	Unit	Notation	Level 1	Level 2	Level 3
Current	Ampere	I	12	17	22
Gap Voltage	Voltage	V	40	50	60
Pulse on time	μs	T_{ON}	2	4	6
Pulse off time	μs	T_{OFF}	5	7	9
Dielectric Pressure	Kg/cm^2	DP	50	75	100

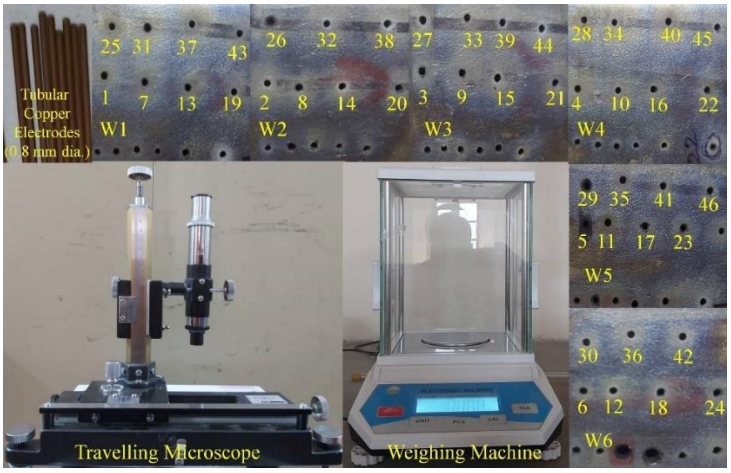

Figure 4 - Actual photographs of copper electrodes, workpieces, electronic weighing machine, and travelling microscope.

Six specimens of size 35 × 35 mm^2 with a uniform thickness of 6.156 mm with a variation of 0.001 mm were used for the experimentation process of EDM drilling with the help of tubular copper electrodes of 0.8 mm diameter. An electronic balance with 0.001 g least count has been used to measure the workpiece's weight and electrode before and after each experiment. The top and bottom diameters of each hole were measured for four different orientations of the hole with the help of a travelling microscope (0.01 mm least count), and the average values were recorded at the end of every experiment. Actual photographs of copper electrodes, workpieces, electronic weighing

machine, and travelling microscope are shown in Figure 4, along with experiment numbers of each hole. Process performance parameters of EDM one can get using Equation 1, 2 & 3.

$$MRR = \frac{(inital-final)weitht\ of\ work\ material}{machining\ time \times desnity\ of\ work\ material} \quad (1)$$

$$TWR = \frac{(inital-final)weitht\ of\ electrode}{machining\ time \times desnity\ of\ electrode} \quad (2)$$

$$DoT = tan^{-1}\left[\frac{D_t - D_b}{2H}\right] \quad (3)$$

D_t and D_b are the average top and bottom diameters, respectively, and H is the hole's depth. Factors and their levels, along with the measured values of MRR, TWR, and DoT, are tabulated in Table 4.

Table 4 - Values of MRR, TWR, and DoT and their GRCs, GRG, and order along with experimental process parameter.

Ex. No.	Factors and their levels					Responses			Grey Relational Coefficient			GRG	Order
	I	V	T_{ON}	T_{OFF}	DP	MRR	TWR	DoT	MRR	TWR	DoT		
1	12	50	4	7	100	0.0110	0.0067	0.0171	0.3786	0.6820	0.6086	0.5564	29
2	17	50	2	5	75	0.0128	0.0047	0.0284	0.4050	0.8364	0.3784	0.5399	32
3	22	50	4	7	100	0.0195	0.0091	0.0130	0.5535	0.5538	0.7777	0.6283	13
4	17	50	4	7	75	0.0149	0.0067	0.0146	0.4419	0.6803	0.6999	0.6074	18
5	17	50	6	5	75	0.0196	0.0065	0.0146	0.5552	0.6929	0.6999	0.6493	8
6	12	50	4	7	50	0.0076	0.0044	0.0154	0.3364	0.8729	0.6666	0.6253	14
7	12	50	4	9	75	0.0084	0.0041	0.0211	0.3455	0.9050	0.4999	0.5835	24
8	17	50	2	7	100	0.0075	0.0053	0.0284	0.3347	0.7805	0.3784	0.4979	40
9	22	50	4	5	75	0.0243	0.0084	0.0300	0.7466	0.5888	0.3590	0.5648	25
10	17	40	2	7	75	0.0094	0.0040	0.0252	0.3572	0.9100	0.4242	0.5638	27
11	17	40	4	7	50	0.0114	0.0046	0.0138	0.3838	0.8539	0.7368	0.6582	7
12	17	60	4	5	75	0.0277	0.0128	0.0268	1.0000	0.4329	0.4000	0.6110	16
13	17	50	6	7	50	0.0147	0.0036	0.0268	0.4390	0.9683	0.4000	0.6024	20
14	17	60	4	7	50	0.0178	0.0151	0.0300	0.5070	0.3794	0.3590	0.4151	44
15	12	50	6	7	75	0.0114	0.0057	0.0106	0.3835	0.7536	0.9333	0.6901	2
16	17	50	4	9	50	0.0091	0.0063	0.0227	0.3540	0.7108	0.4666	0.5105	38
17	12	60	4	7	75	0.0171	0.0171	0.0187	0.4895	0.3442	0.5599	0.4645	42
18	12	50	2	7	75	0.0098	0.0042	0.0268	0.3622	0.8912	0.4000	0.5511	30
19	22	50	4	7	50	0.0181	0.0062	0.0276	0.5147	0.7114	0.3889	0.5383	33
20	17	60	2	7	75	0.0126	0.0131	0.0268	0.4025	0.4252	0.4000	0.4092	45
21	17	40	4	9	75	0.0074	0.0045	0.0187	0.3341	0.8630	0.5599	0.5857	23
22	17	50	2	7	50	0.0107	0.0048	0.0268	0.3740	0.8290	0.4000	0.5343	34
23	22	50	6	7	75	0.0164	0.0064	0.0097	0.4736	0.6980	1.0000	0.7239	1
24	17	40	4	7	100	0.0143	0.0052	0.0122	0.4313	0.7933	0.8235	0.6827	3
25	17	40	4	5	75	0.0144	0.0046	0.0154	0.4324	0.8475	0.6666	0.6489	9
26	22	60	4	7	75	0.0222	0.0174	0.0171	0.6469	0.3392	0.6086	0.5316	35
27	17	50	4	7	75	0.0156	0.0068	0.0235	0.4563	0.6736	0.4516	0.5271	36
28	22	50	2	7	75	0.0175	0.0045	0.0325	0.4990	0.8616	0.3333	0.5646	26
29	17	50	4	5	50	0.0174	0.0045	0.0260	0.4959	0.8610	0.4117	0.5895	22
30	17	50	4	7	75	0.0203	0.0073	0.0122	0.5797	0.6423	0.8235	0.6818	4
31	17	50	4	7	75	0.0157	0.0049	0.0317	0.4587	0.8225	0.3415	0.5409	31

32	17	50	4	7	75	0.0124	0.0062	0.0300	0.3988	0.7157	0.3590	0.4912	41
33	12	50	4	5	75	0.0112	0.0053	0.0284	0.3814	0.7814	0.3784	0.5137	37
34	22	40	4	7	75	0.0208	0.0046	0.0325	0.5940	0.8534	0.3333	0.5936	21
35	17	50	2	9	75	0.0075	0.0049	0.0317	0.3345	0.8218	0.3415	0.4992	39
36	17	50	4	7	75	0.0083	0.0047	0.0138	0.3441	0.8414	0.7368	0.6407	12
37	17	60	4	9	75	0.0186	0.0178	0.0300	0.5273	0.3333	0.3590	0.4065	46
38	12	40	4	7	75	0.0074	0.0033	0.0211	0.3333	1.0000	0.4999	0.6111	15
39	17	50	6	9	75	0.0147	0.0051	0.0146	0.4389	0.8059	0.6999	0.6483	10
40	17	50	4	5	100	0.0191	0.0052	0.0154	0.5429	0.7913	0.6666	0.6669	6
41	17	60	4	7	100	0.0211	0.0154	0.0146	0.6060	0.3741	0.6999	0.5600	28
42	17	50	4	9	100	0.0145	0.0070	0.0122	0.4344	0.6647	0.8235	0.6408	11
43	22	50	4	9	75	0.0153	0.0084	0.0130	0.4513	0.5866	0.7777	0.6052	19
44	17	40	6	7	75	0.0152	0.0041	0.0154	0.4480	0.9036	0.6666	0.6727	5
45	17	50	6	7	100	0.0218	0.0053	0.0260	0.6322	0.7833	0.4117	0.6091	17
46	17	60	6	7	75	0.0203	0.0158	0.0244	0.5794	0.3667	0.4375	0.4612	43

Mathematical modelling has been performed to establish the relationship between variable control parameters of EDM and response parameters (viz. MRR, TWR, and DoT).

Complicated interrelationships between designated performance characteristics are effectively analyzed with GRA's help as it gives an efficient solution to discrete uncertainty and multi-input data problems (Datta et al., 2008; Gautam & Mishra, 2019). Data processing was carried out by normalizing the results obtained from the experimentation. It has been used for multi-response optimization of MRR, TWR, and DoT. First, the performance characteristics were normalized: MRR has been normalized for larger the better using Equation 4, and TWR and DoT have been normalized for smaller the better using Equation 5.

For larger the better performance characteristic:

$$x_i = \frac{y_i - \min(y_i)}{\max(y_i) - \min(y_i)} \quad (4)$$

For smaller the better performance characteristic:

$$x_i = \frac{\max(y_i) - y_i}{\max(y_i) - \min(y_i)} \quad (5)$$

Where y_i is the i^{th} response, and $\max(y_i)$ and $\min(y_i)$ are the maximum and minimum values of the responses.

Before finding the value of gray relational coefficients (GRC) using Equation 7, the deviational sequences were evaluated using Equation 6, and gray relational grades (GRG) were assessed using Equation 8 tabulated and its order shown in Table 4.

$$\Delta x_i = \max(x_i) - x_i \quad (6)$$

$$\xi_i = \frac{\min(\Delta x_i) + \zeta \max(\Delta x_i)}{\Delta x_i + \zeta \max(\Delta x_i)} \quad (7)$$

Where Δx_i is the deviation sequence and ζ = 0.5 (equal preference for all performance parameters).

Based on GRG, the overall evaluation of multi-performance characteristics is evaluated as GRG as a weighting sum of GRCs.

$$\gamma_i = \frac{1}{n}\sum_1^n \xi_i \quad (8)$$

Comparability sequence exerts over the reference sequence as GRG indicates the degree of influence, and its more immense value indicates that the quality of product complements the outstanding value.

Taguchi optimization technique is recognized for one response at a time approach. The multi-response optimization using Taguchi was carried out with the assistance of GRA. Taguchi considers the signal to noise ratio (SNR) as the quality characteristic of the response. According to the quality

characteristics, the SNRs (Taguchi & Phadke, 1989) were calculated using Equation 9 or 10 and tabulated in Table 5.

For larger the better:

$$\eta = -10 \times log_{10} \frac{1}{n} \sum_1^n \left(\frac{1}{y_i^2} \right) \quad (9)$$

For smaller the better:

$$\eta = -10 \times log_{10} \frac{1}{n} \sum_1^n y_i^2 \quad (10)$$

Table 5 - S/N ratio for various response parameters and GRG.

Ex. No.	S/N Ratio			
	MRR	**TWR**	**DoT**	**GRG**
1	-39.1615	43.4957	35.3630	-5.0919
2	-37.8776	46.5048	30.9276	-5.3531
3	-34.1974	40.7786	37.7247	-4.0362
4	-37.7934	44.1744	32.9920	-4.8807
5	-34.1713	43.7137	36.7017	-3.7505
6	-42.3359	47.1967	36.2322	-4.0781
7	-41.4752	47.8006	33.5084	-4.6797
8	-42.5127	45.4353	30.9276	-6.0580
9	-32.3018	41.5498	30.4452	-4.9618
10	-40.5358	47.8954	31.9812	-4.9776
11	-38.8771	46.8359	37.1981	-3.6334
12	**-31.1461**	37.8620	31.4384	-4.2796
13	-36.6480	48.9940	31.4384	-4.4021
14	-34.9818	36.3935	30.4452	-7.6361
15	-38.8931	44.9137	39.5280	-3.2212
16	-40.7751	44.0713	32.8649	-5.8407
17	-35.3397	35.3397	34.5730	-6.6598
18	-40.1811	47.5407	31.4384	-5.1754
19	-34.8362	44.0842	31.1792	-5.3789
20	-37.9863	37.6585	31.4384	-7.7606
21	-42.5723	47.0093	34.5730	-4.6465
22	-39.4286	46.3644	31.4384	-5.4440
23	-35.7015	43.8168	40.2232	-2.8069
24	-36.8944	45.6811	38.2852	-3.3156
25	-36.8575	46.7158	36.2322	-3.7571
26	-33.0883	35.1831	35.3630	-5.4887
27	-	-	-	-
28	-35.1399	46.9814	29.7684	-4.9646
29	-35.2047	46.9702	31.7055	-4.5901
30	-	-	-	-
31	-	-	-	-
32	-	-	-	-
33	-39.0079	45.4523	30.9276	-5.7856
34	-33.6557	46.8265	**29.7684**	-4.5305
35	-42.5354	46.2259	29.9882	-6.0340
36	-	-	-	-
37	-34.6128	**34.9989**	30.4452	-7.8179
38	-42.6580	49.5937	33.5084	-4.2779
39	-36.6488	45.9240	36.7017	-3.7649

40	-34.3579	45.6434	36.2322	-3.5183
41	-33.5151	36.2395	36.7017	-5.0359
42	-36.7948	43.1432	38.2852	-3.8650
43	-36.2819	41.5002	37.7247	-4.3621
44	-36.3765	47.7740	36.2322	-3.4434
45	-33.2329	45.4885	31.7055	-4.3066
46	-33.8389	36.0218	32.2659	-6.7227
Note: As there are six center points, the S/N ratio of Exp. No. 4 only is available				

The significance of individual process parameters and their effects on the performance characteristics by decomposing the variance of the relative impact of different factors are evaluated using ANOVA as it indicates the impact of the control parameters on the GRA. The ANOVA analysis of GRA has been done, and the obtained results are tabulated in Table 6, which shows that the V and TON are the most significant process parameter.

Table 6 - Analysis of variance of GRG.

Source	SS	DF	Mean Square	F-value	p-value
Model	0.1814	20	0.0091	2.71	0.0098
A (I)	0.0015	1	0.0015	0.4456	0.5105
B (V)	0.0837	1	0.0837	24.99	< 0.0001
C (T_{ON})	0.0503	1	0.0503	15.01	0.0007
D (T_{OFF})	0.0058	1	0.0058	1.73	0.2006
E (DP)	0.0085	1	0.0085	2.53	0.1240
AB	0.0018	1	0.0018	0.5336	0.4719
AC	0.0001	1	0.0001	0.0304	0.8630
AD	0.0002	1	0.0002	0.0644	0.8017
AE	0.0063	1	0.0063	1.88	0.1821
BC	0.0008	1	0.0008	0.2423	0.6269
BD	0.0050	1	0.0050	1.49	0.2337
BE	0.0036	1	0.0036	1.08	0.3085
CD	0.0004	1	0.0004	0.1172	0.7349
CE	0.0005	1	0.0005	0.1388	0.7126
DE	0.0007	1	0.0007	0.2092	0.6513
A^2	0.0007	1	0.0007	0.1980	0.6601
B^2	0.0081	1	0.0081	2.42	0.1324
C^2	0.0000	1	0.0000	0.0107	0.9183
D^2	0.0000	1	0.0000	0.0090	0.9252
E^2	0.0003	1	0.0003	0.1000	0.7544
Residual	0.0838	25	0.0034		
Lack of Fit	0.0567	20	0.0028	0.5253	0.8613
Pure Error	0.0270	5	0.0054		
Total	0.2651	45			

3. Results and discussions

Interaction and main effect plots for MRR are shown in Figure 5 & 6, respectively. It is evident that by increasing the discharge current, MRR increases to an average value of 0.0193 g/min due to the liberation of higher energy in the spark gap, which raises melting and evaporation of the workpiece material. The behaviour of gap voltage on MRR is the same as that of the discharge current, and it reaches an average value of 0.0197 g/min, as enhancement in the gap voltage leads to the rise in heat intensity. MRR increases to an average of 0.0168 g/min with a surge in T_{ON}, whereas T_{OFF} has a reverse impact on the MRR; its average value falls from 0.183 - 0.0119 g/min. T_{ON} and T_{OFF} indicate the sparking rate; when the sparking rate rises, more heat will carry from one spark to the other, which increases the MRR. The influence of dielectric pressure DP has a direct impact on MRR. By increasing DP, efficient flushing of the molten metal occurs, which increases the average value of MRR to 0.0161g/min. The discharge current is the significant control variable parameter for maximizing MRR.

Figure 7 & 8 show the interaction and main effect plots for TWR, respectively. These figures indicate that the TWR increases to the average of 0.0081 g/min by increasing the discharge current. It is because of enhancement in the spark energy, which leads to a higher temperature of the electrode. The gap voltage has a higher impact on TWR and raises it to an average of 0.0156 g/min, which is around nine times compared to the effect of discharge current. This massive jump in TWR is because of the direct relation between gap voltage and total energy of discharge in one spark. In contrast, the other control factors such as T_{ON}, T_{OFF}, and DP have minor impacts on TWR. For minimal TWR, gap voltage is the most significant control parameter.

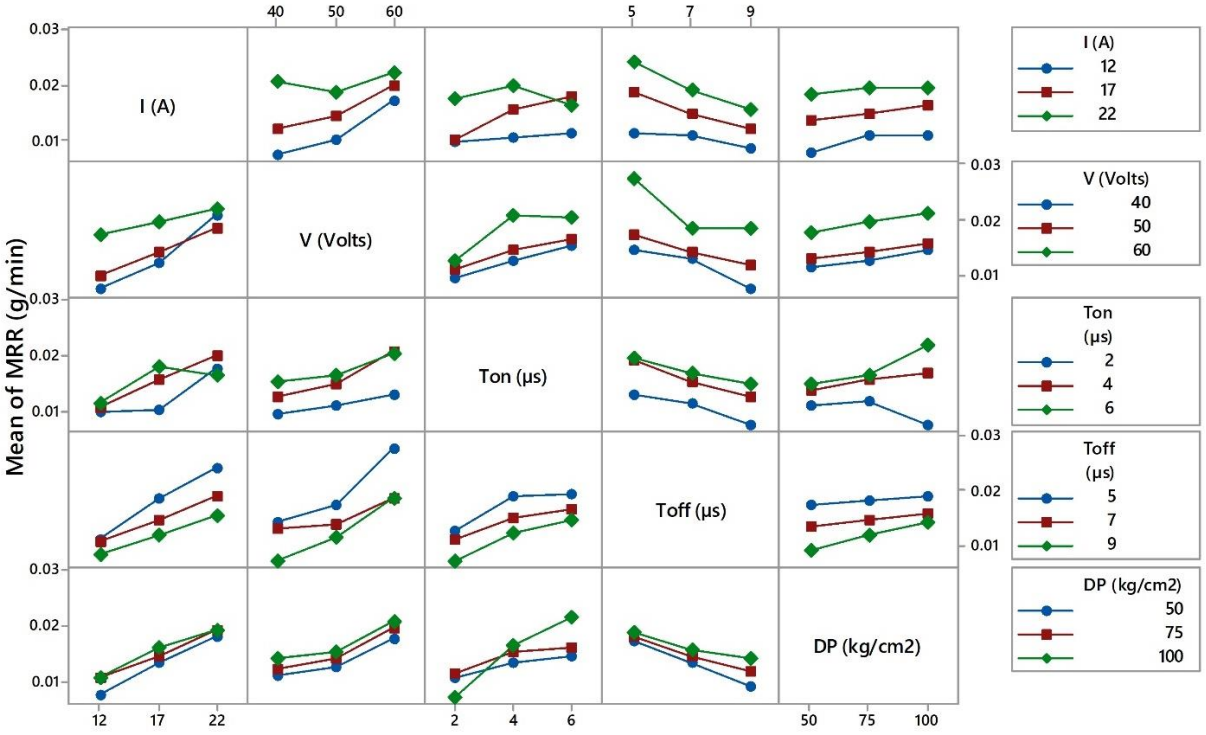

Figure 5 - Interaction plot of process parameters for MRR.

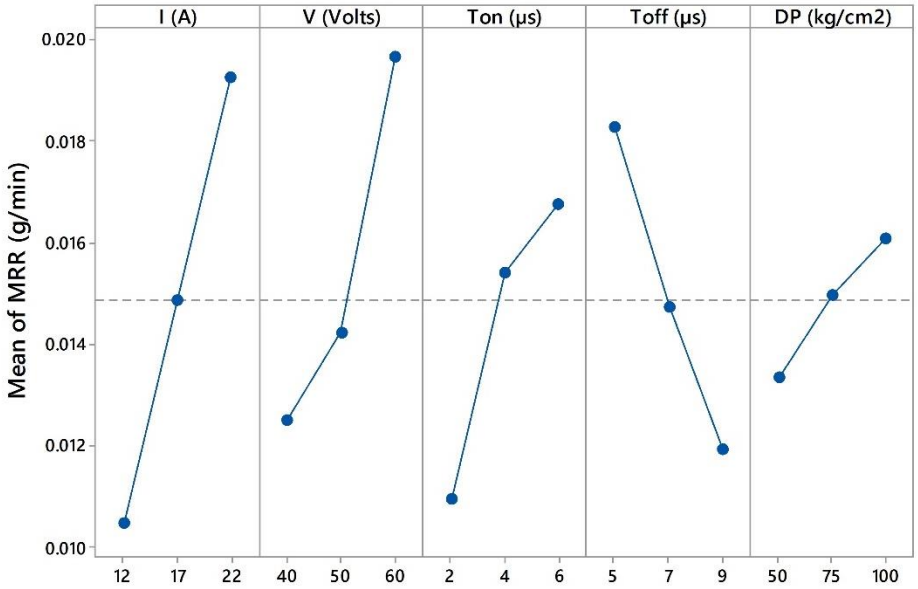

Figure 6 - Main effect plot for MRR.

Figure 9 & 10 show the interaction and main effect plot for DoT, respectively. These plots indicate that by increasing the discharge current and the gap voltage, the DoT increased by 10 & 21 %, respectively, due to the spark's total discharge energy. By increasing T_{ON}, T_{OFF}, and DP, the value of DoT decreased by around 37, 11 & 26 %, respectively, because of an increase in discharge time and cooling of the workpiece material. As DoT needs to be minimized, T_{ON} is the most influencing process parameter followed by DP.

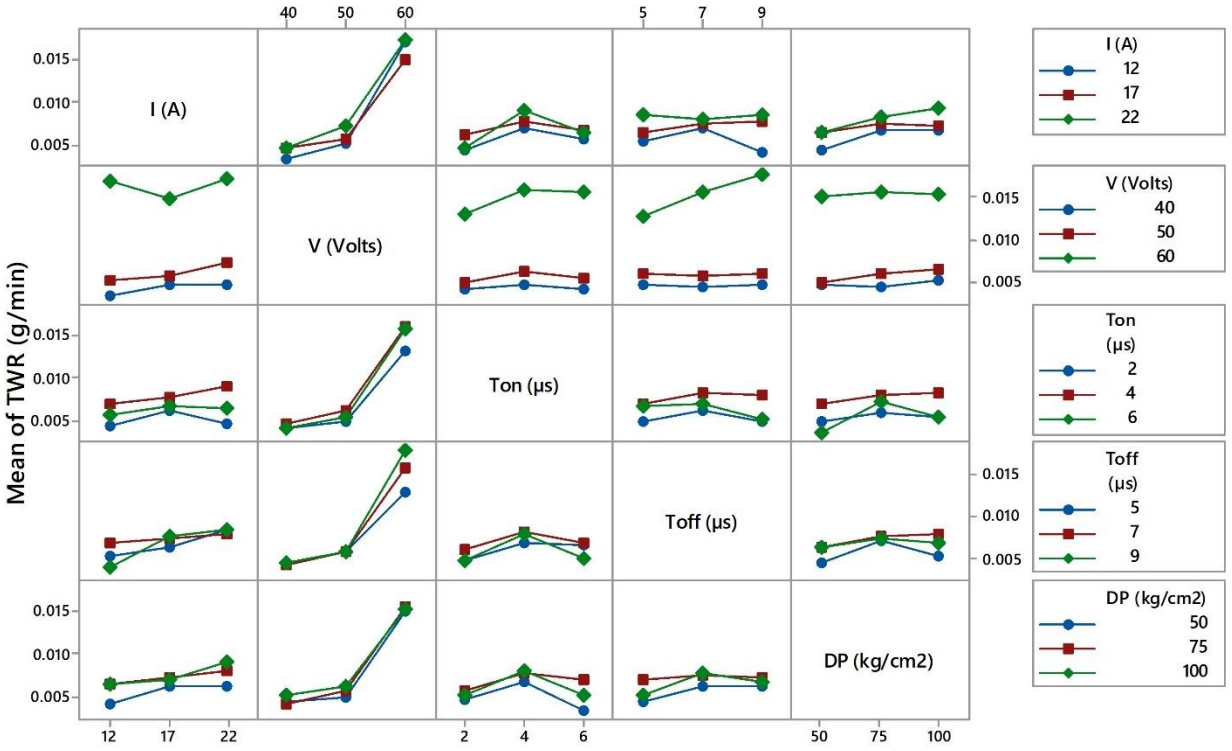

Figure 7 - Interaction plot of process parameters for TWR.

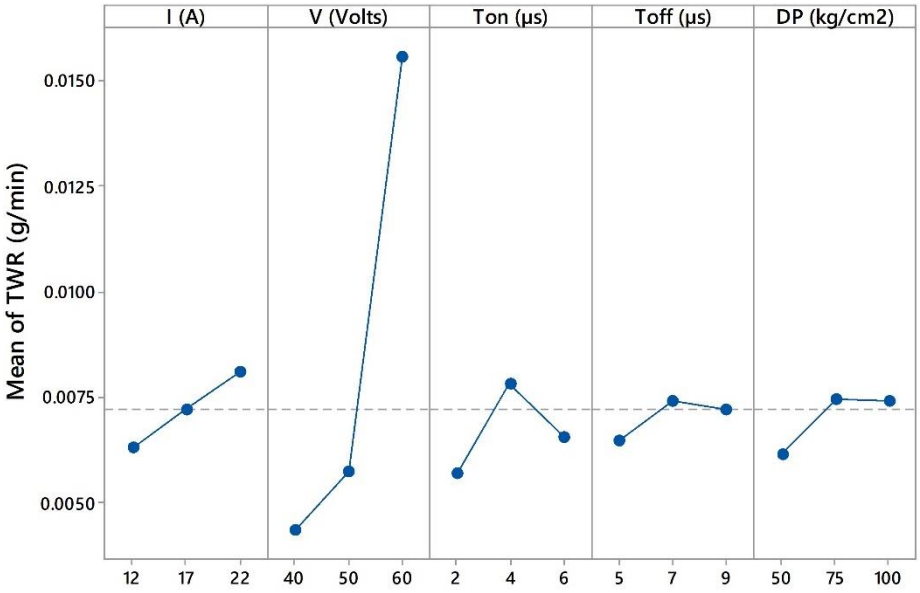

Figure 8 - Main effect plot for TWR.

Figure 11, 12 & 13 shows the surface and contour plots for MRR, TWR and DoT, respectively, as functions of the most significant control variable parameters (viz. viz. V and T_{ON}), at I = 22 A, T_{OFF} = 7 µs and DP = 100 kg/cm2. Figure 11 indicates that the maximum value of MRR is 0.0277 g/min at higher gap voltage & discharge time, and the minimum value is 0.0074 g/min at lower gap voltage & discharge time. This variation occurs due to energy availability.

Figure 12 indicates that the maximum and minimum values of TWR are 0.0177 and 0.0033 g/min, respectively. Gap voltage has a more significant influence on it, whereas T_{ON} has the most negligible impact. Maximum TWR is at a higher value of gap voltage as the energy received by the electrode from the spark will rise. Figure 13 indicates that the DoT has its maximum and minimum values of 0.032 and 0.01 radians, respectively. The DoT has a higher value nearer to the lower values of gap voltage and the discharge time, whereas it is low at higher values of gap voltage and discharge time. A minimum value will occur if the sparking will concentrate at the electrode's tip, leading to the material removal for getting the hole drilled.

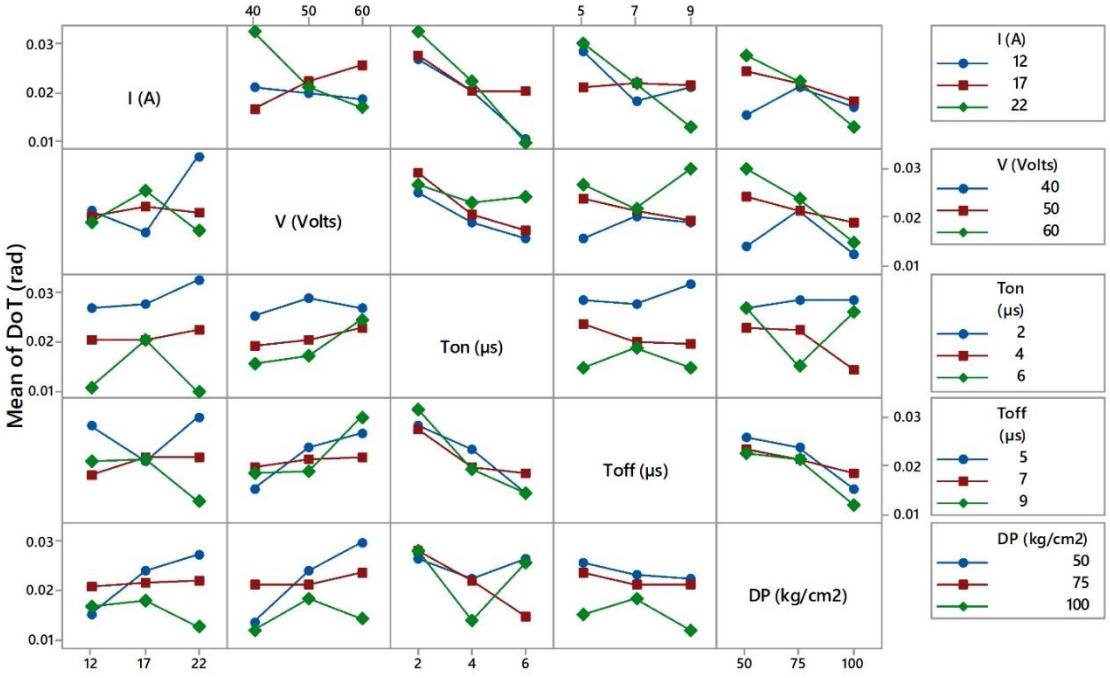

Figure 9 - Interaction plot of process parameters for DoT.

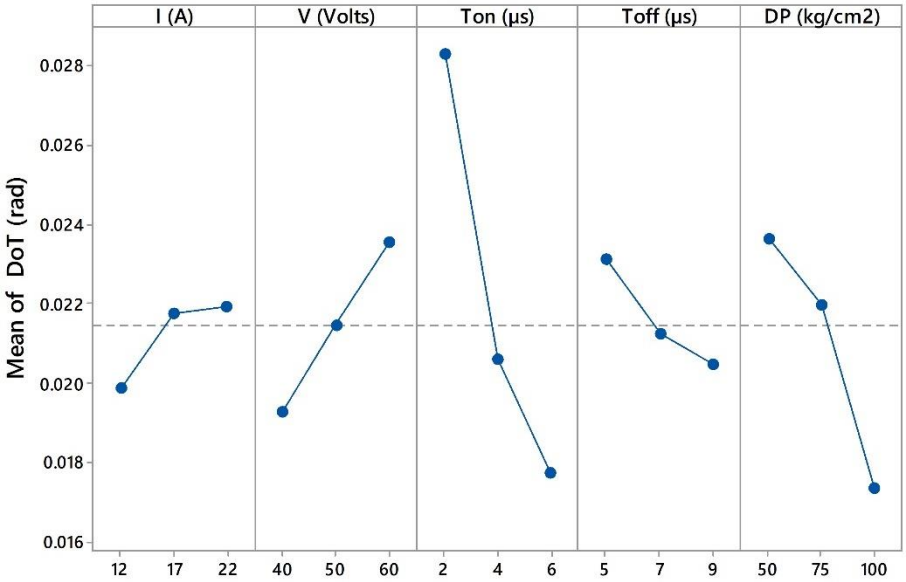

Figure 10 - Main effect plot for DoT.

A confirmation test has been carried out to validate performance characteristics' improvement after obtaining optimum control parameters of EDM, and optimal value has been evaluated using Equation 13.

$$\eta_{est} = \eta_m + \sum_1^n (\eta_i - \eta_m) \quad (13)$$

Where η_m & η_i are the mean and i^{th} response, respectively.

L_{23} is found as the optimum conditions for maximizing MRR and minimizing TWR & DoT from the GRG and its order simultaneously. The optimum combination of process control variable parameters are I_3, V_2, T_{ON3}, T_{OFF2} & DP_2, and their responses are MRR 0.0164 g/min, TWR 0.0064 g/min, DoT 0.0097 radians & SNR of GRG -2.8069 dB.

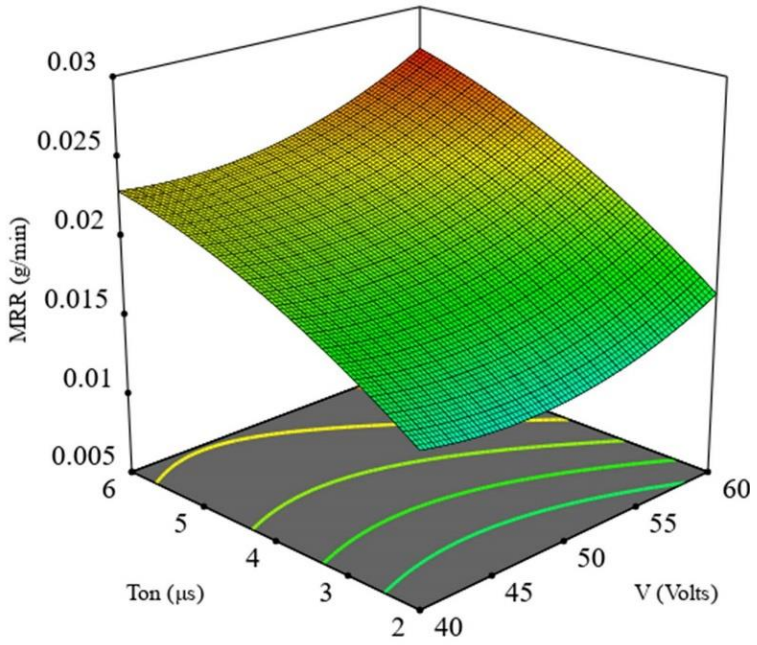

Figure 11 - Surface and contour plots for MRR.

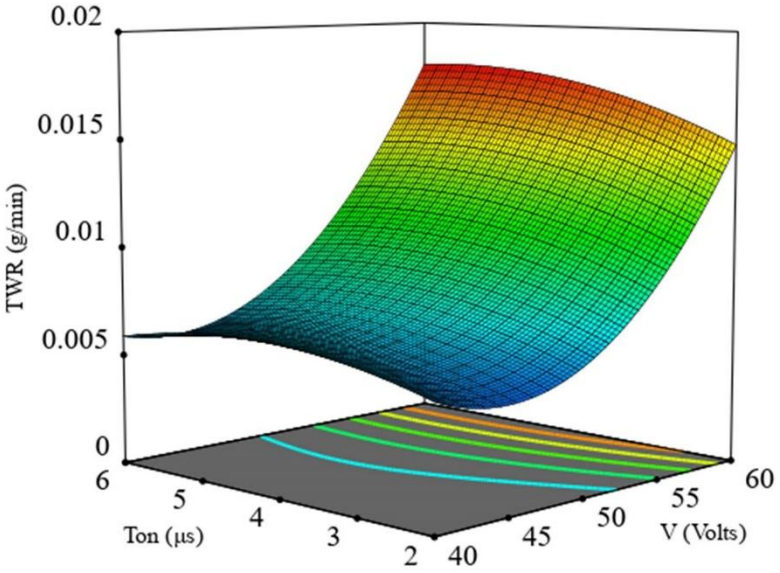

Figure 12 - Surface and contour plots for TWR.

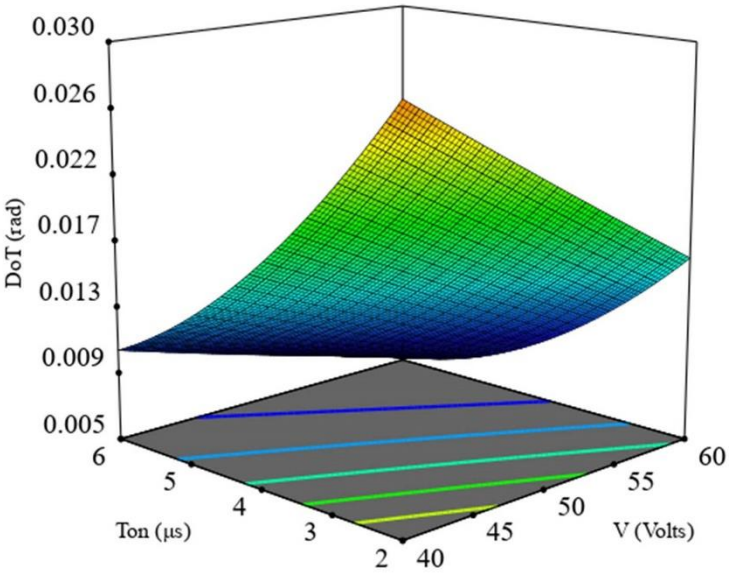

Figure 13 - Surface and contour plots for DoT.

It has been observed that the optimum setting of input control parameters, comparing with the initial set, that there are improvements in the quality characteristics. MRR was raised by 49.1 %, where TWR and DoT were lowered by 4.5 and 43.3 %.

4. Conclusions

Based on the experimentation of EDM drilling on Nitinol SMA and its analysis using GRG assisted Taguchi for multi-response optimization of the quality characteristics (viz. MRR, TWR, and DoT), the following conclusions can be made:

i. Gap voltage and discharge time are the most significant process control variables.
ii. The optimum frame of parameters is higher discharge current (I) and time (T_{ON}) with average gap voltage (V), charging time (T_{OFF}) (higher than T_{ON}), and dielectric flushing pressure (DP).
iii. MRR, TWR, and DoT are improved by 49.1, 4.5, and 43.3 %, respectively, compared to the initial experiment.

References

Ahmed, A., Lew, M. T., Diwakar, P., Kumar, A. S., & Rahman, M. (2019). A novel approach in high performance deep hole drilling of Inconel 718. *Precision Engineering*, *56*(January), 432–437. https://doi.org/10.1016/j.precisioneng.2019.01.012

Al-Amin, M., Abdul Rani, A. M., Abdu Aliyu, A. A., Abdul Razak, M. A., Hastuty, S., & Bryant, M. G. (2020). Powder mixed-EDM for potential biomedical applications: A critical review. *Materials and Manufacturing Processes*, *00*(00), 1–23. https://doi.org/10.1080/10426914.2020.1779939

Chakraborty, S., Sudhakar Dandge, S., & Agarwal, S. (2019). Non-traditional machining processes selection and evaluation: A rough multi-attributive border approximation area comparison approach. *Computers & Industrial Engineering*, *139*(July 2019), 106201. https://doi.org/10.1016/j.cie.2019.106201

Datta, S., Bandyopadhyay, A., & Pal, P. K. (2008). Grey-based taguchi method for optimization of bead geometry in submerged arc bead-on-plate welding. *The International Journal of Advanced Manufacturing Technology*, *39*(11–12), 1136–1143. https://doi.org/10.1007/s00170-007-1283-6

Deepan Bharathi Kannan, T., Pegada, R., Sathiya, P., & Ramesh, T. (2018). A comparison of the effect of different heat treatment processes on laser-welded NiTinol sheets. *Journal of the Brazilian Society of Mechanical Sciences and Engineering*, *40*(12), 562. https://doi.org/10.1007/s40430-018-1481-1

Gautam, G., & Mishra, D. (2019). Evaluation of geometrical quality characteristics in pulsed Nd:YAG laser cutting of Kevlar-29/Basalt fiber reinforced hybrid composite using Grey relational analysis based on genetic algorithm. *FME Transactions*, *47*(3), 560–575. https://doi.org/10.5937/fmet1903560G

HuuPhan, N., Muthuramalingam, T., Vu, N. N., & Tuan, N. Q. (2020). Influence of micro size titanium powder-mixed dielectric medium on surface quality measures in EDM process. *International Journal of Advanced Manufacturing Technology*, *109*(3–4), 797–807. https://doi.org/10.1007/s00170-020-05698-9

Jahan, M. P., Rahman, M., & Wong, Y. S. (2011). A review on the conventional and micro-electrodischarge machining of tungsten carbide. *International Journal of Machine Tools and Manufacture*, *51*(12), 837–858. https://doi.org/10.1016/j.ijmachtools.2011.08.016

Kumar, D., Singh, N. K., & Bajpai, V. (2020). Recent trends, opportunities and other aspects of micro-EDM for advanced manufacturing: a comprehensive review. *Journal of the Brazilian Society of Mechanical Sciences and Engineering*, *42*(5), 1–26. https://doi.org/10.1007/s40430-020-02296-4

Kumar, S., Ghoshal, S. K., Arora, P. K., & Nagdeve, L. (2020). Multi-variable optimization in die-sinking EDM process of AISI420 stainless steel. *Materials and Manufacturing Processes*, *00*(00), 1–11. https://doi.org/10.1080/10426914.2020.1843678

Lin, J. L., & Lin, C. L. (2002). The use of the orthogonal array with grey relational analysis to optimize the electrical discharge machining process with multiple performance characteristics. *International Journal of Machine Tools and Manufacture*, *42*(2), 237–244. https://doi.org/10.1016/S0890-6955(01)00107-9

Liu, J. F., Li, C., Fang, X. Y., Jordon, J. B., & Guo, Y. B. (2018). Effect of wire-EDM on fatigue of nitinol shape memory alloy. *Materials and Manufacturing Processes*, *33*(16), 1809–1814. https://doi.org/10.1080/10426914.2018.1512125

Majumder, H., & Maity, K. (2018). Prediction and optimization of surface roughness and micro-hardness using grnn and MOORA-fuzzy-a MCDM approach for nitinol in WEDM. *Measurement*, *118*, 1–13. https://doi.org/10.1016/j.measurement.2018.01.003

Mwangi, J. W., Bui, V. D., Thüsing, K., Hahn, S., Wagner, M. F. X., & Schubert, A. (2020). Characterization of the arcing phenomenon in micro-EDM and its effect on key mechanical properties of medical-grade Nitinol. *Journal of Materials Processing*

Technology, *275*(March 2019), 116334. https://doi.org/10.1016/j.jmatprotec.2019.116334

Mwangi, J. W., Weisheit, L., Bui, V. D., Zanjani, M. Y., & Schubert, A. (2018). Influence of Micro-EDM on the Phase Transformation Behaviour of Medical-Grade Nitinol. *Shape Memory and Superelasticity*, *4*(4), 450–461. https://doi.org/10.1007/s40830-018-00195-1

Sarmah, A., Kar, S., & Patowari, P. K. (2020). Surface modification of aluminum with green compact powder metallurgy Inconel-aluminum tool in EDM. *Materials and Manufacturing Processes*, *35*(10), 1104–1112. https://doi.org/10.1080/10426914.2020.1765253

Sharma, A., & Yadava, V. (2018). Experimental analysis of Nd-YAG laser cutting of sheet materials – A review. *Optics and Laser Technology*, *98*, 264–280. https://doi.org/10.1016/j.optlastec.2017.08.002

Sharma, P., Singh, S., & Mishra, D. R. (2014). Electrical Discharge Machining of AISI 329 Stainless Steel Using Copper and Brass Rotary Tubular Electrode. *Procedia Materials Science*, *5*, 1771–1780. https://doi.org/10.1016/j.mspro.2014.07.367

Shin, M.-C., Kim, Y.-S., Cheong, H.-G., & Chu, C.-N. (2019). Performance of a TR-iso-pulse generator in micro ED-drilling. *Precision Engineering*, *June 2018*, 0–1. https://doi.org/10.1016/j.precisioneng.2019.01.013

Singh, P. N., Raghukandan, K., & Pai, B. C. (2004). Optimization by Grey relational analysis of EDM parameters on machining Al–10%SiCP composites. *Journal of Materials Processing Technology*, *155–156*(1–3), 1658–1661. https://doi.org/10.1016/j.jmatprotec.2004.04.322

Singh, R., Dvivedi, A., & Kumar, P. (2020). EDM of high aspect ratio micro-holes on Ti-6Al-4V alloy by synchronizing energy interactions. *Materials and Manufacturing Processes*, *35*(11), 1188–1203. https://doi.org/10.1080/10426914.2020.1762207

Sonawane, S. A., & Kulkarni, M. L. (2018). Optimization of machining parameters of WEDM for Nimonic-75 alloy using principal component analysis integrated with Taguchi method. *Journal of King Saud University - Engineering Sciences*, *30*(3), 250–258. https://doi.org/10.1016/j.jksues.2018.04.001

Taguchi, G., & Phadke, M. S. (1989). Quality Engineering through Design Optimization. In *Quality Control, Robust Design, and the Taguchi Method* (pp. 77–96). Springer US. https://doi.org/10.1007/978-1-4684-1472-1_5

Tripathy, S., & Tripathy, D. K. (2016). Multi-attribute optimization of machining process parameters in powder mixed electro-discharge machining using TOPSIS and grey relational analysis. *Engineering Science and Technology, an International Journal*, *19*(1), 62–70. https://doi.org/10.1016/j.jestch.2015.07.010

Vidyasagar, K. E. C., Rana, A., & Kalyanasundaram, D. (2020). Optimization of laser parameters for improved corrosion resistance of nitinol. *Materials and Manufacturing Processes*, 1–9. https://doi.org/10.1080/10426914.2020.1784926